Journal of Molecular Catalysis A: Chemical 352 (2012) 21–30

Contents lists available at ScienceDirect

Journal of Molecular Catalysis A: Chemical

journal homepage: www.elsevier.com/locate/molcata

Transition metal coordination polymers MeX_2(4,4′bipyridine) (Me = Co, Ni, Cu; X = Cl^-, CH_3OCO^-, acetylacetonate) selective catalysts for cyclohexene epoxidation with molecular oxygen and isobutyraldehyde

Emilian Angelescu[a], Octavian D. Pavel[a], Rodica Ionescu[a], Ruxandra Bîrjega[b], Mihaela Badea[c], Rodica Zăvoianu[a,*]

[a] University of Bucharest, Faculty of Chemistry, Department of Organic Chemistry, Biochemistry and Catalysis, 4-12 Bd. Regina Elisabeta, Bucharest 3, 030018, Romania
[b] National Institute for Lasers, Plasma and Radiation Physics, P. O. Box Mg – 27; Măgurele, Bucharest, Romania
[c] University of Bucharest, Faculty of Chemistry, Department of Inorganic Chemistry, 4-12 Bd. Regina Elisabeta, Bucharest 3, 030018, Romania

ARTICLE INFO

Article history:
Received 1 February 2011
Received in revised form 27 July 2011
Accepted 5 August 2011
Available online 12 August 2011

Keywords:
Co coordination polymers
Ni coordination polymers
Cu coordination polymers
4,4′-bipyridine
Supramolecular materials
Cyclohexene epoxidation
Mukayiama reaction

ABSTRACT

This paper presents aspects concerning the catalytic activity of several transition metal coordination polymers with the general formula $^2{}_\infty$[Me(II)X_2(4,4′bipyridine)] (Me(II) = Co, Ni, Cu; X = Cl^-, CH_3OCO^-, and acetylacetonate) towards the epoxidation of cyclohexene with molecular oxygen in the presence of isobutyraldehyde as reductant. The obtained results proved that all the investigated catalysts showed a high selectivity for epoxidation (over 88%). The conversion of cyclohexene was found to depend on the nature of both the transition metal cation and the ligand X. The most active catalyst was found to be $^2{}_\infty$[Co(II)$(CH_3OCO)_2$(4,4′bipyridine)].

1. Introduction

Transition-metal coordination polymers are important supramolecular materials with possible applications as catalysts, advanced materials such as liquid crystals, sensors or materials with magnetic or non-linear optic properties. Such solids obtained from different types of molecular building blocks have also molecular sieving and ion-exchange properties [1–3]. These compounds containing redox active ions of transition metals such as Fe, Co, Ni, Cu, Mn, and V may have catalytic activity for reactions following a redox mechanism. The catalytic oxidation of olefins is an economically important process for the obtaining of different fine chemicals intermediates such as epoxides, ketones and allylic alcohols depending upon the oxidation agent, the nature of the catalysts and the reaction conditions employed. Hydrogen peroxide, tert-butylhydroperoxide, and oxygen may be used as oxidation agents. Transition metal complexes represent an important category of redox catalysts for these oxidation processes. These catalysts may be classified as: (i) soluble complexes, (ii) heterogeneous catalysts containing transition metal complexes grafted on different supports such as silica or functionalized polymers, and (iii) transition metal coordination polymers. The oxidation may follow either a direct path when using the oxidation agent, the redox catalyst and the substrate or an indirect path when a reductant agent such as an aldehyde or a nitrile is also introduced in the reaction mixture. Up to now, the catalytic activity of the transition metal coordination polymers has been tested only in reactions taking place via the direct path. The selectivity of the transformation into different reaction products varies with the nature of the polymeric structure used as catalyst. Several examples are presented as it follows. Thus, for the oxidation of cyclohexene with tert-butyl hydroperoxide, terephthalato-bridged tetranuclear polymeric Ni^{II} complex [4], polymeric oxovanadium(IV) complexes with Schiff bases [5] and an extended Cu^{II}-organic framework containing dihydrogen benzene-1,2,4,5-tetracarboxylate anions and 2,2′-bipyridine are selective catalysts for the epoxidation [6], while under similar reaction conditions a polymeric Schiff base Cu^{II} complex is more selective to allylic oxidation products [7].

The oxidation of cyclohexene to 1,2-epoxycyclohexane using H_2O_2 as oxidation agent may be realised using Mn(II) dicarboxylate coordination polymer catalysts and imidazole

* Corresponding author.
E-mail address: rodicazavoianu@gmail.com (R. Zăvoianu).

1381-1169/$ – see front matter © 2011 Published by Elsevier B.V.
doi:10.1016/j.molcata.2011.08.001

[8], or Mn_2L complexes (L = 4-[2-[2-(1,1,1,5,5,5-hexafluoro-4-oxopentylideneamino)ethylamino]ethylimino] - 1,1,1,5,5,5 - hexafluoropentan-2-one) and CH_3COONH_4 [9]. The oxidation of cyclohexene with H_2O_2 in the presence of a polymer complex of 2-thiomethylbenzimidazole-polystyrene with $Cu(CH_3COO)_2$ is selective for cyclohexane-1,2-diol formation [10], while in the presence of polymeric Schiff base copper(II) complex, the main reaction products are cyclohexenone, and cyclohexenol [7].

The direct oxidations of cyclohexene with oxygen are selective towards the formation of allylic oxidation products on polymer-bound 2,2′-bipyridine cobalt complexes [11], on a copper metal–organic framework [Cu(4,4′-bipyridine)$(H_2O)_2(BF_4)_2$(4,4′-bipyridine)] [12] and in the presence of a polymeric Schiff base copper(II) complex [7].

The Mukaiyama oxidation of alkenes with oxygen in the presence of aldehydes for the obtaining of the corresponding epoxides under mild conditions [13] is an example for the oxidations taking place via the indirect path which requires the presence of a reductant in the reaction mixture. Until now, the reports concerning this reaction mention the catalytic activity of different metal complex catalysts such as β-diketonates [14–16], complexes containing Schiff-base ligands [17], Ru(II)-complexes [18,19], immobilized porphyrinatomanganese(III) [20], mononuclear complexes of phenoxyacetic acid derivatives and Schiff bases with Co(II) or Cu(II) [21], or bis-triphenylphosphine-dichlorocobalt (II) and benzyltriphenyl phosphonium-tetrachlorocobaltate [22]. Up to now, there were no reports regarding the catalytic activity of non-soluble transition-metal coordination polymers with 4,4′-bipyridine (4,4′-bpy) bridging ligands for this type of reaction.

Coordination polymers like $^2{}_\infty$[Me(II)Cl_2(4,4′-bpy)] (Me(II) = Fe, Co, Ni) [1] were synthesized and structurally characterized nearly 15 years ago. They are thermally stable up to 400 °C, insoluble in water and usual organic solvents. These polymeric structures have regular shaped inner cavities surrounded by 4,4′-bpy units (Fig. 1). Due to these properties, these solids were expected to be catalysts with high stability and shape-selectivity. However, since in the scientific literature stream, there is a lack of information concerning their catalytic activity, we thought important to show that these metals and ligands can also work as catalysts in coordination polymers.

Therefore the main goal of this paper is to investigate the catalytic activity and selectivity of the polymeric metal-complexes $^2{}_\infty$[Me(II)Cl_2(4,4′-bpy)] (Me(II) = Co, Ni, Cu) in Mukaiyama epoxidation of cyclohexene using molecular oxygen as oxidizing agent and isobutyraldehyde as reductant. The effect induced by the replacement of chlorine ligand with acetate (CH_3OCO^-) or acetylacetonate ($C_5H_7O_2$) in the structure of the solid displaying the highest catalytic activity is also investigated.

2. Experimental

2.1. Synthesis of catalysts

The synthesis of $^2{}_\infty$[Me(II)Cl_2(4,4′-bpy)] catalyst was performed according to the procedure reported by Lawandy et al. [1] using chemically pure Merck reagents. Thus, a stoichiometric mixture of $CoCl_2 \times 6H_2O$ (1 mmol), and 4,4′-bpy (1 mmol) in 8 mL water was heated in 25 mL acid digestion bomb at 170 °C for 3 days. The product is a single phase pale pink purplish polycrystalline solid which was filtered, washed with water and acetone, then dried in air.

The same procedure was applied when using $NiCl_2 \times 6H_2O$, and $CuCl_2 \times 4H_2O$ as bivalent transition metal source. $^2{}_\infty$[$NiCl_2$(4,4′-bpy)] is pale green–yellowish, while $^2{}_\infty$[$CuCl_2$(4,4′-bpy)] is blue–green.

[$Co(OCOCH_3)_2$(4,4′-bpy)$(H_2O)_2$] was synthesized according to the method developed by Zhang et al. [2] by preparing a methanol solution of 4,4′-bpy (1 mmol) which was slowly added under stirring to a methanol solution of $Co(OCOCH_3)_2 \times 4H_2O$ (1 mmol). A light orange precipitate was formed immediately and was separated by filtration.

The same method was used to synthesize [$Co(C_5H_7O_2)_2$(4,4′-bpy)] using methanol solution of cobalt acetylacetonate as cobalt source. The polymeric complex is yellow.

2.2. Catalysts characterization

The catalysts were characterized by chemical and elemental analysis. The determination of the metal content was performed by Atomic Absorption Spectrometry on Pye-Unicam AAS Spectrometer. N and C were determined by elemental analysis on Carlo Erba automatic analyzer. Cl content was determined by volumetric analysis of the solution used for the absorption of the gases evolved during the combustion of the samples using Schöniger method.

The as-synthesized complexes were characterized by DR UV–vis-NIR in the range 210–1500 nm. The spectra were recorded using a Jasco V670 spectrometer equipped with an integration sphere. MgO was used as white reference.

The XRD patterns were collected on a PANalytical X'PERT MPD theta–theta system in continuous scan mode (counting 2 s per 0.02° θ) ranging from 5° to 75° 2θ. A Ni filter, a curved monochromator and a programmable divergence slit enabling constant sampling area irradiation were placed in the diffracted beam (λ = 0.15418 nm). Data were analyzed using the PANalytical X'PERT High Score Plus software package. The Scherrer formula was used to evaluate the crystallite sizes.

These characterization techniques have been used in order to verify the composition and the structure of the complexes prepared by us according to the methods developed by Lawandy et al. [1] and Zhang et al. [2].

2.3. Catalytic tests

The catalysts were tested in the epoxidation of cyclohexene with molecular oxygen using isobutyraldehyde as reductant and acetonitrile as solvent. In a typical experiment, 40 mg of complex catalyst were contacted with cyclohexene (0.08 mol) and isobutyraldehyde (0.16 mol) which were solved in 20 mL acetonitrile. All reagents had been freshly distilled. The reactions were carried out during 7 h at room temperature and 1 atmosphere of O_2 in a sealed stirred flask (250 mL) provided with a manometer and an admission tube connected to the oxygen pressurized cylinder. Prior to the admission of the catalyst in the flask, the system was purged with oxygen in order to remove the air. During the experiment, the oxygen from the pressurized cylinder was introduced in the flask at the surface level of the reaction mixture in order to maintain the pressure at 1 atmosphere as indicated by the manometer.

The reaction products were monitored hourly using a GC K072320 Thermo-Quest chromatograph equipped with FID detector and a capillary column of 30 m length with DB5 stationary phase. The oxidation products were identified by comparison with standard samples (retention time in GC), and by mass spectrometer-coupled chromatography using a GC–MS Varian Saturn 2100 T equipped with a CP-SIL 8 CB Low Bleed/MS column of 30 m length and 0.25 mm diameter. The results of the chromatographic analysis enabled us to evaluate the cyclohexene conversion and to calculate the selectivity to epoxide and by-products. The epoxide yield was calculated as the product of cyclohexene conversion and selectivity to epoxide.

The catalytic tests for the determination of the recyclability and the leaching of the catalysts have been performed using tenfold the amount of catalyst, reagents and solvent (e.g. 0.4 g of catalyst, cyclohexene (0.8 mol), isobutyraldehyde (1.6 mol), 200 mL

Table 1
The chemical composition of the polymeric coordination complexes catalysts.

Complex catalysts	% Cl		Me (II) (%)		% C		% H		% N	
	Calc.	Exp.	Calc.	Exp.	Calc.	Exp.	Calc.	Exp.	Calc.	Exp.
$^2_\infty$[$CoCl_2$(4,4′-bpy)]	24.82	25.08	20.63	21.04	41.96	42.46	2.8	2.14	9.79	9.28
$^2_\infty$[$Co(OCOCH_3)_2$(4,4′-bpy) × $(H_2O)_2$]	–		15.98	14.82	45.53	42.24	4.88	5.33	7.59	7.04
$^2_\infty$[$Co(C_5H_7O_2)_2$(4,4′-bpy)]	–		14.29	14.54	58.11	59.48	5.33	4.94	6.78	6.11
$^2_\infty$[$NiCl_2$(4,4′-bpy)]	24.85	24.58	20.55	21.10	42.00	42.86	2.80	2.22	9.80	9.24
$^2_\infty$[$CuCl_2$(4,4′-bpy)]	24.44	24.52	21.87	22.30	41.30	42.02	2.75	2.04	9.64	9.12

acetonitrile). This modification of the reaction conditions was required for the recovery of a sufficient amount of spent catalyst to be used for the determination of metal content by AAS and for XRD analyses. After 7 h reaction time the catalyst was separated from the reaction mixture. The recovered catalyst was washed with acetone and dried in air for 24 h. After drying, the solid was used in the next reaction cycle. Five reaction cycles were performed for each catalyst in order to investigate their recyclability. For the leaching tests, the recovered liquid reaction mixture was introduced again in the reactor and maintained under 1 atmosphere of O_2 during 7 h in the absence of the catalyst. The analysis of the reaction mixture after the tests performed in the presence of the catalyst and after the catalyst was removed allowed us to estimate the contribution of the homogeneous catalysis, due to the leaching of metal species.

3. Results and discussion

3.1. Catalysts characterization

3.1.1. Chemical composition

The chemical compositions of the catalysts as determined by elemental analysis, AAS for metal content and Schőniger method for Cl content are presented in Table 1.

The data in Table 1 show that for $^2_\infty$[Me(II)Cl_2(4,4′-bpy)] (Me(II) = Co, Ni, Cu) and $^2_\infty$[$Co(C_5H_7O_2)_2$(4,4′-bpy)] compounds there is a good agreement between the calculated and experimental values. For $^2_\infty$[$Co(OCOCH_3)_2$(4,4′-bpy) × $(H_2O)_2$], the poor agreement between the experimental and calculated values of concentrations is probably due to an uncompleted drying of the sample submitted to the analysis.

3.1.2. Characterization by XRD

There are only few literature data concerning the powder X-ray diffraction patterns of transition metals polymeric coordination compounds such as $^2_\infty$[Me(II)Cl_2(4,4′-bpy)]. The PDF4+ (2009) database provided by the International Centre for Diffraction Data-ICDD contains JCPDFS files for $C_{10}H_8Cl_2N_2Ni$ (050-2049) and $C_{10}H_8Cl_2N_2Cu$ (050-2051), respectively [23]. The corresponding structural data were presented by Masciocchi et al. [24].

As it may be seen in Fig. 2, the X-ray diffraction patterns of our samples $^2_\infty$[$NiCl_2$(4,4′-bpy)] (chemical formula $C_{10}H_8Cl_2N_2Ni$) and $^2_\infty$[$CuCl_2$(4,4′-bpy)] (chemical formula $C_{10}H_8Cl_2N_2Cu$) are similar to the simulated X-ray patterns of the standards included in ICDD database.

Four polycrystalline compounds $^2_\infty$[$MeCl_2$(4,4′-bpy)], Me = Ni, Co, Mn and Co/Ni synthesized by Lawandy et al. [1] and characterized using XRD have been found to be isostructural all exhibiting an orthorhombic symmetry, spatial group C*mmm*. The transition metal ion is placed in octahedral environment; the *b* axis corresponds to the polymeric chain, while the *c* axis corresponds to the stacking of the polymeric chains through Cl^- ions bridges connected to the metal ions.

For all the powder samples of $^2_\infty$[Me(II)Cl_2(4,4′-bpy)], Me(II) = Ni, Co, Cu, prepared in this study, the X-ray diffraction patterns presented in Fig. 3 are similar, indicating the formation of isostructural structures. Excepting a decrease of

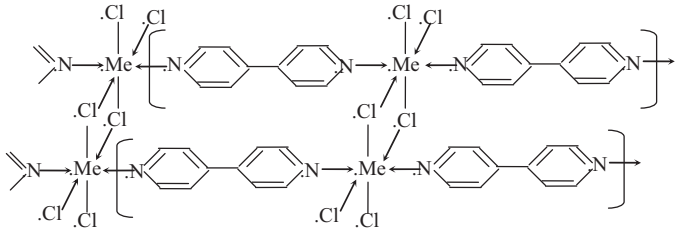

Fig. 1. One-dimensional covalently linked chain in $^2_\infty$[$MeCl_2$(4,4′-bpy)] (M = Fe, Co, Ni).

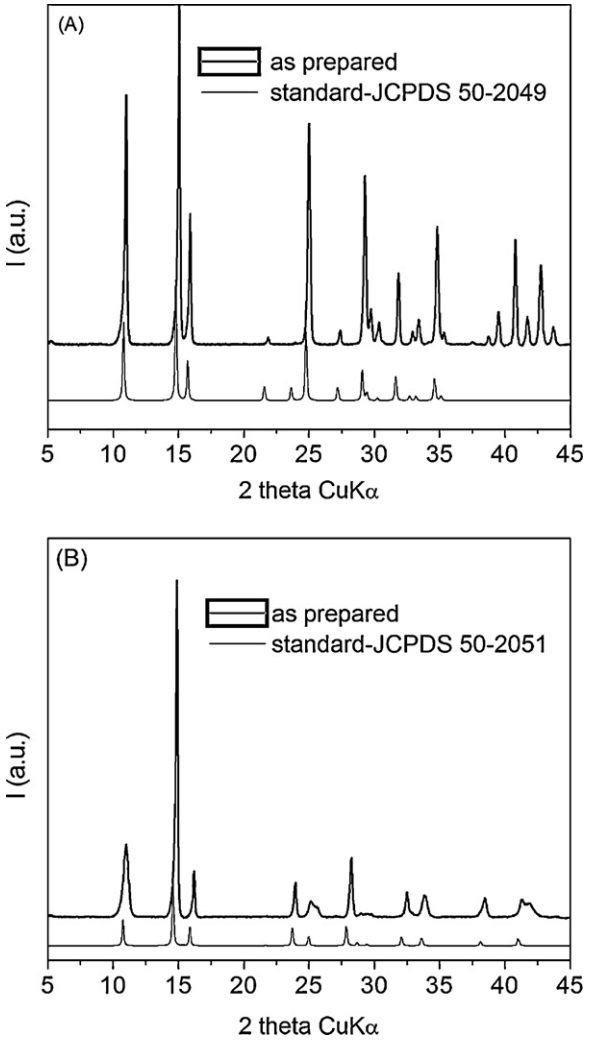

Fig. 2. (A) XRD pattern of $^2_\infty$[$NiCl_2$(4,4′-bpy)]; (B) XRD pattern of $^2_\infty$[$CuCl_2$(4,4′-bpy)].

Table 2
Lattice parameters and cystallite sizes.

Sample	Schannon ionic radii (Å)	a (Å)	b (Å)	c (Å)	Vol (Å^3)	D_{200} (nm)	D_{020} (nm)	D_{001} (nm)
$^2_\infty$[NiCl$_2$(4,4′-bpy)]	0.69	11.76	11.20	3.56	469	101	90	74
$^2_\infty$[CuCl$_2$(4,4′-bpy)	0.73	11.90	10.94	3.715	485	98	122	65.5
$^2_\infty$[CoCl$_2$(4,4′-bpy)]	0.745	11.96	11.41	3.62	494	116	191	120

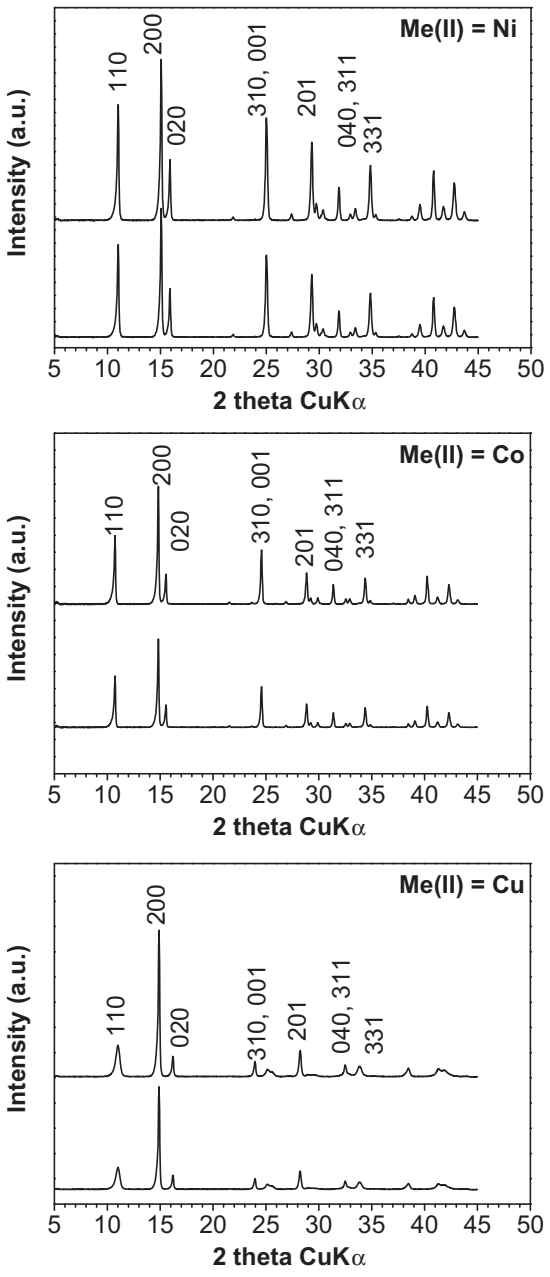

Fig. 3. XRD patterns of $^2_\infty$[Me(II)Cl$_2$(4,4′-bpy)], (Me(II) = Ni, Co, Cu); black lines – fresh catalysts; grey lines – catalysts after 5 reaction cycles.

the intensity of the diffraction maxima, there are no significant differences between the diffraction patterns of the fresh catalysts and those recorded after their use in five reaction cycles. This fact indicates a good stability of the catalysts under reaction conditions. Taking into account the similarity of the recorded patterns and the standard patterns, the diffraction maxima have been Miller indexed according to the literature standard structural data as orthorhombic symmetry, space group C*mmm*. Considering the

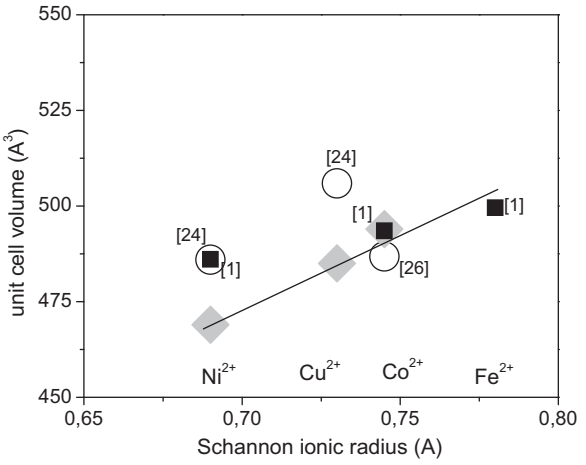

Fig. 4. The effect of Schannon ionic radius on the unit cell volume: ◈ experimental data; ○ data from references [14,17]; ■ data from reference [1].

particular orientation of the polymeric chain along *b* direction, the crystallite sizes have been determined for the 3 crystallographic directions using the (2 0 0), (0 2 0) and (0 0 1) reflections.

The lattice parameters and crystallites sizes are presented in Table 2.

The structural data show that the crystalline frameworks are similar and, as expected, the volume of the unit cell depends on the ionic radius of the transition metal.

Fig. 4, which includes also the values presented in literature, displays the effect of the dimension of the Schannon ionic radius [25] in octahedral environment. For $^2_\infty$[CoCl$_2$(4,4′-bpy)] the values obtained for the sample prepared in this study are almost identical with those obtained by Lawandy et al. [1] and Feyerherm et al. [26] namely a = 11.954 Å, b = 11.411 Å and c = 3.618 Å.

Fig. 5 displays the PXRD patterns of $^2_\infty$[Co(OCOCH$_3$)$_2$(4,4′-bpy)] and $^2_\infty$[Co(C$_5$H$_7$O$_2$)$_2$(4,4′-bpy)] complexes compared to $^2_\infty$[CoCl$_2$(4,4′-bpy)]. It may be noticed that the three patterns are quite different suggesting a different mode of linking of Co(4,4′-bpy) chains. Also, as it was the case for $^2_\infty$[CoCl$_2$(4,4′-bpy)], there

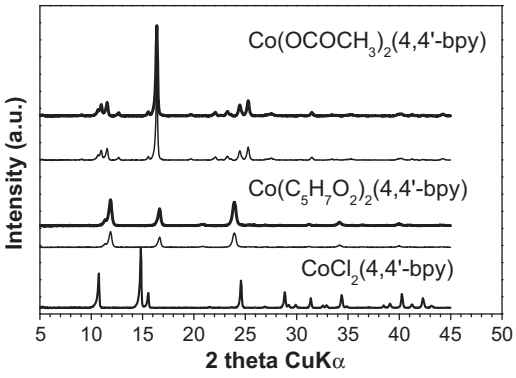

Fig. 5. PXRD patterns of $^2_\infty$[Co(CH$_3$OCO)$_2$(4,4′-bpy)] and $^2_\infty$[Co(C$_5$H$_7$O$_2$)$_2$(4,4′-bpy)] compared to $^2_\infty$[CoCl$_2$(4,4′-bpy)]. Thick lines – fresh catalysts, thin lines – catalysts after 5 reaction cycles.

Table 3
XRD data (Bragg angles, corresponding interplanar distances and relative intensities).

$Co(OCOCH_3)_2$(4,4′-bpy)			$Co(acac)_2$(4,4′-bpy)		
2 theta CuKα	*d* (Å)	*I* rel	2 theta CuKα	*d* (Å)	*I* rel
10.65	8.31	5	11.46	7.72	21
10.97	8.07	12	11.88	7.45	100
11.53	7.67	13	16.54	5.36	27
12.67	6.99	3	16.67	5.32	49
15.55	5.70	3	20.82	4.27	5
16.38	5.41	100	23.93	3.72	1
19.70	4.51	2	25.37	3.51	3
22.07	4.03	4	25.83	3.45	2
23.26	3.82	5	26.98	3.30	2
24.47	3.64	11	31.20	2.78	5
25.28	3.52	17	33.98	2.64	2
27.46	3.25	2	34.18	2.62	11
31.48	2.84	4	34.31	2.61	2
35.24	2.55	1	36.42	2.47	3
40.09	2.25	2	39.97	2.26	7
41.23	2.19	2	40.95	2.20	2
44.25	2.05	2	44.10	2.05	2

are no significant alterations in the diffraction patterns of the catalysts $^2{}_\infty[Co(OCOCH_3)_2(4,4'\text{-bpy})]$ and $^2{}_\infty[Co(C_5H_7O_2)_2(4,4'\text{-bpy})]$ used in five reaction cycles. There are no standard diffraction data for powders of $^2{}_\infty[Co(OCOCH_3)_2(4,4'\text{-bpy})]$ and $^2{}_\infty[Co(C_5H_7O_2)_2(4,4'\text{-bpy})]$ or for similar compounds with other transition metals in the available ICDD database (PDF4+, 2009). There is a report by Zhang et al. [2] claiming a monoclinic symmetry (space group P2/*n*) for $^2{}_\infty[Co(OCOCH_3)_2(4,4'\text{-bpy})]$ monocrystal. That could be the case for the as-above prepared powder $^2{}_\infty[Co(OCOCH_3)_2(4,4'\text{-bpy})]$ for which the XRD patterns reveals a complicated structure of low symmetry, probably monoclinic or anorthic. It is worth mentioning that we did not detect any diffraction lines issued from the raw materials used for the syntheses $C_{10}H_8N_2$-4.4′-dipyridyl (JCPDS No. 24-1998) and $Co(CH_3CO_2)_2{\cdot}4H_2O$ (JCPDS No. 25-0372) and/or $Co(Co_5H_7O_2)_2{\cdot}2H_2O$ (JCPDS No. 30-1605). The positions of the diffraction lines (2θ), their corresponding interplanar distances (*d*) and relative intensities for the powders of the prepared compounds are presented in Table 3.

3.1.3. Characterization by DR-UV–vis NIR

The solid state d–d spectrum of the nickel complex (Fig. 6) shows the characteristic bands of Ni(II) in a pseudo-octahedral environment. The absorptions at 8300, 13,900 and 24,210 cm^{-1} are assigned to the spin allowed $^3A_{1g} \rightarrow {}^3T_{2g}$, $^3A_{1g} \rightarrow {}^3T_{1g}$ (F) and $^3A_{1g} \rightarrow {}^3T_{1g}$ (P) transitions. The shoulder at 12,390 cm^{-1} can be assigned to the spin forbidden transition $^3A_{1g} \rightarrow {}^1E_g$. The bands are broad as a result of the different nature of the ligands that lead to a distortion from a regular octahedral stereochemistry. The value of the splitting parameter 10 *Dq* of 8300 cm^{-1} is very close to the medium value for the chromophore $[NiN_2Cl_4]$ of 8400 cm^{-1}. The Racach parameter of 0.85 indicates a lower degree of covalence.

For the Co complexes, the main d–d transitions bands are presented in Table 4. For $^2{}_\infty[CoCl_2(4,4'\text{-bpy})]$ and $^2{}_\infty[Co(OCOCH_3)_2(4,4'\text{-bpy})]$, the aspect of the spectra (Fig. 6) indicates a tetragonal environment of Co(II), while for $^2{}_\infty[Co(C_5H_7O_2)_2(4,4'\text{-bpy})]$ a stereochemistry closer to octahedral is more probable.

Since the ground term for the d^7 octahedral high spin configuration is $^4T_{1g}$ (which in the case of tetragonal distortion splits in ^4E_g and $^4A_{2g}$), the parameter 10 *Dq* cannot be determined directly from the energy of one band alone [27]. The values of ν_1, ν_2, allow the calculation of the splitting parameter, 10 *Dq* as being equal to the difference (ν_2–ν_1). According to the molecular orbital theory,

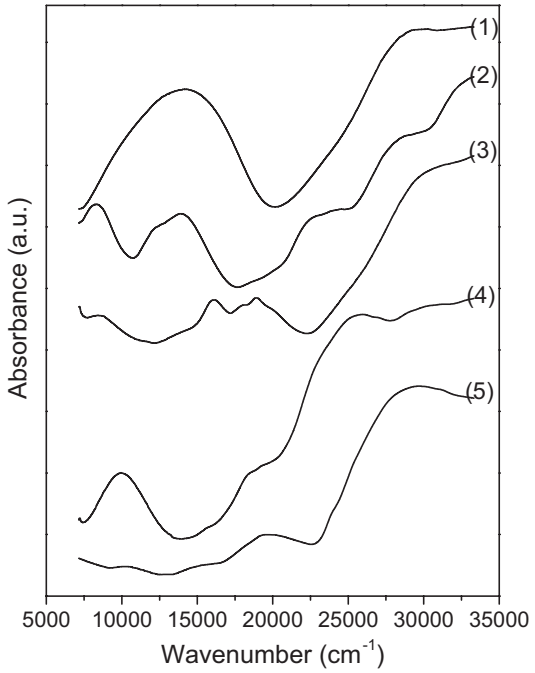

Fig. 6. DR-UV–vis NIR spectra of $^2{}_\infty[Me(II)Cl_2(4,4'\text{-bpy})]$ complexes; 1 – Me(II) = Cu; 2 – Me(II) = Ni; 3 – Me(II) = Co; 4 – $^2{}_\infty[Co(C_5H_7O_2)_2(4,4'\text{-bpy})]$; 5 – $^2{}_\infty[Co(OCOCH_3)_2(4,4'\text{-bpy})]$.

the value of 10 *Dq* will depend upon the extent of the overlapping between the orbitals of the metal and those of the ligand. A higher value of the 10 *Dq* parameter is correlated with a stronger metal–ligand bond.

The electronic spectrum of the copper complex (Fig. 6) shows a broad band centered at 14,200 cm^{-1} assigned to d_{xz}, $d_{yz} \rightarrow d_x2_{-y}2$ in agreement with an octahedral surrounding [28,29].

3.1.4. Catalytic tests results

When discussing the obtained results, one should bear in mind that besides ethylene, the epoxidation of olefins with molecular oxygen in the presence of an aldehyde reductant is possible according to two different reaction pathways [30,31]:

i) Non catalytic epoxidation, which is a slow reaction carried out following a mechanism related to aldehyde auto oxidation as it was described by Kaneda et al. [32] and Lassila et al. [33] (Scheme 1).
ii) Catalytic epoxidation in the presence of catalysts containing a transition metal with redox properties following the Mukaiyama–Yamada mechanism [13,34–38]. The catalytic process is fast and even at room temperature 100% selectivity to epoxides and high conversions of the alkenes may be obtained.

For both reaction pathways, the first stage (Eq. (1)) is the generation of an acyl radical, which is further oxidized to an acylperoxo radical [30]:

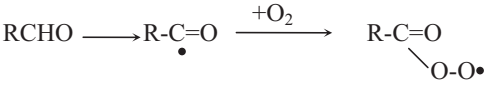

(1)

The generation of the acyl radical in the catalytic method may be realized either following a redox mechanism determined by the ability of the transition metal ion to undergo modifications of its oxidation state as described by Eq. (2) or following a radicalic mechanism [14,39,40] promoted by the ability of the transition metal ion to coordinate oxygen forming metal–oxygen-radical species which

Table 4
Splitting parameters and d–d transition bands for the investigated Co(II) complexes.

Co(II) complex	ν_1 (cm^{-1})		ν_2 (cm^{-1})		ν_3 (cm^{-1})	10 Dq (cm^{-1})
	$^4E_g \rightarrow {}^4E_g$	$^4E_g \rightarrow {}^4B_{2g}$	$^4E_g \rightarrow {}^4A_{2g}$	$^4E_g \rightarrow {}^4E_g$	$^4E_g \rightarrow {}^4B_{1g}, {}^4A_{2g}$	
$^2{}_\infty$[$CoCl_2$(4,4′-bpy)]	8390 ν_{1med} = 8448	8565	18,900 ν_{2med} = 18,347	18,070	16,095	9899
$^2{}_\infty$[$Co(C_5H_7O_2)_2$(4,4′-bpy)]	9900		19,600 ν_{2med} = 18,993	18,690	15,750	9093
$^2{}_\infty$[$Co(OCOCH_3)_2$(4,4′-bpy)]	10,415		19,600 ν_{2med} = 18,880	18,520	15,500	8465

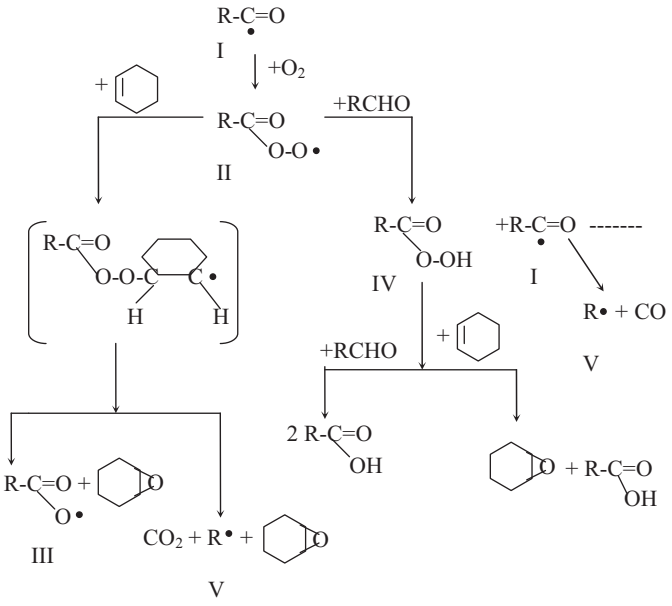

Scheme 1. Non-catalytic reaction pathway for the epoxidation of cyclohexene with molecular oxygen in the presence of an aldehyde.

may abstract the hydrogen from the aldehyde molecule generating an acyl radical as described by Eq. (3).

$$RCHO + (Lm)Me^{+n} \xrightarrow{-H^+} R\text{–}\dot{C}{=}O + (Lm)Me^{(n+1)+} \quad (2)$$

$$Me^{+n} \rightarrow (Me\text{–}O\text{–}\dot{O})^{+n} \xrightarrow{+n+RCHO} (Me - O - OH)^{+n} + R\text{–}\dot{C}{=}O \quad (3)$$

The transformation of the aldehyde through the pathway described by Eq. (2) or the one described by Eq. (3) depends upon the nature of the transition metal ion in the catalyst and its ability to adopt different oxidation states. The reduction of the high oxidation states of the transition metal ion by the aldehyde used as reductant agent in the process usually favors the pathway described by Eq. (3).

Scheme 1 presents the possibilities for the formation of the reaction products and the corresponding intermediates when the peroxidation process is performed in the absence of the catalysts as it was proposed by Kaneda et al. [32] and Lassila et al. [33]. As it may be seen in Scheme 1, there are different radical reaction

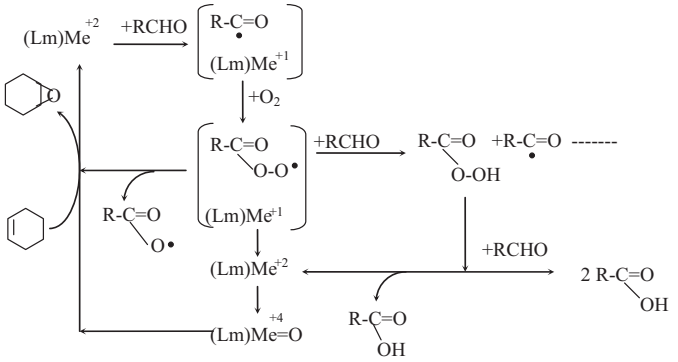

Scheme 3. Epoxidation of cyclohexene with molecular oxygen in the presence of an aldehyde over transition metal catalysts.

intermediates that may be formed during the transformation such as: acyl (I), peroxyacyl (II), oxyacyl (III), peroxyacid (IV), and alkyl (V). In an oxidant environment, the alkyl radical may generate alkyl-peroxides or alkyl-hydroperoxides. All these intermediates may undergo parallel or consecutive transformations which lead to the decrease of the selectivity to 1,2-epoxycyclohexane. Since cyclohexene possess also a high susceptibility of oxidation in allylic position, the oxidation at the double bond may also be accompanied by the allylic oxidation besides the above mentioned secondary reactions as described in Scheme 2 proposed by Wentzel et al. [14,30].

When the epoxidation of cyclohexene is carried out in the presence of a catalyst containing transition metal cations, the reaction intermediates may be temporarily associated to the metallic redox sites, and their possibilities to evolve following different reaction pathways become limited. Meanwhile, as it is presented in Scheme 3, positive consequences towards the increase of the selectivity for the obtaining of the corresponding epoxide do appear.

The catalytic tests for the epoxidation of cyclohexene using transition metal coordination polymers $^2{}_\infty$[Me(II)Cl_2(4,4′-byp)] (Me(II) = Co, Cu, Ni) as catalysts were performed under identical reaction conditions as it was described in Section 2.3. The obtained results are presented in Figs. 7 and 8. The results of a blank test performed under the same reaction conditions in the absence of the catalyst after 7 h were as it follows: conversion of cyclohexene 10.1%, selectivity to 1,2-epoxycyclohexane 68.9%, yield to 1,2-epoxycyclohexane 6.9%. The results of the blank test compared

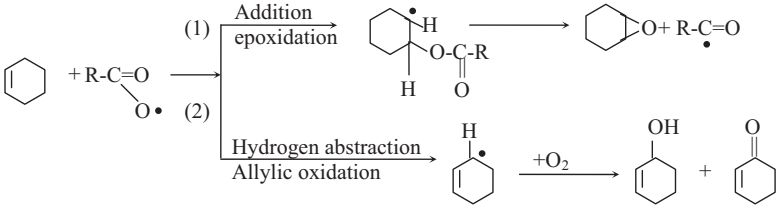

Scheme 2. Non-catalytic epoxidation of cyclohexene and allylic oxidation.

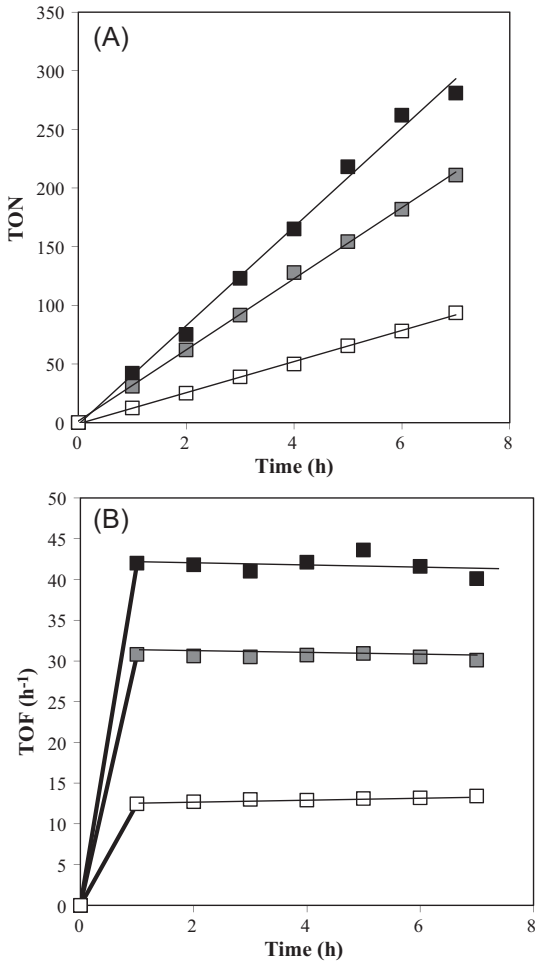

Fig. 7. Temporal variation of the catalytic activity expressed as TON – (A) and TOF – (B) for $^{2}{}_{\infty}$[Me(II)Cl_2(4,4′-bpy)] catalysts Me(II) = Co ■; Me(II) = Ni ■; Me(II) = Cu □; reaction conditions: 40 mg catalyst, 0.08 mol cyclohexene, 0.16 mol isobutyraldehyde, 20 mL acetonitrile solvent, T = 25 °C, p_{O_2} = 1 atm.

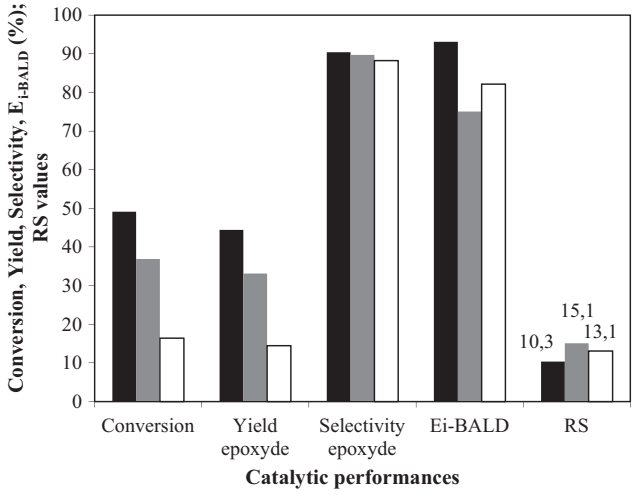

Fig. 8. Catalytic performances of $^{2}{}_{\infty}$[Me(II)Cl_2(4,4′-bpy)] catalysts Me(II) = Co ■; Me(II) = Ni ■; Me(II) = Cu □; reaction conditions: 40 mg catalyst, 0.08 mol cyclohexene, 0.16 mol isobutyraldehyde, 20 mL acetonitrile solvent, 7 h reaction time, T = 25 °C, p_{O_2} = 1 atm.

to those obtained in the presence of the transition metal coordination polymers clearly prove the catalytic activity of the investigated materials. The temporal variation of the catalytic activity expressed as turnover numbers (TON), calculated as the ratio between the number of moles of cyclohexene transformed and the number of redox sites, depends on the transition metal cation following the order: $TON_{Co} > TON_{Ni} > TON_{Cu}$ and indicates a reaction route involving a redox mechanism (Scheme 3). This temporal variation has a linear trend during the first 7 h reaction time as it may be seen in Fig. 7(A).

As it may be seen in Fig. 7(B), when the catalytic activity is expressed as turnover frequency, TOF (number of moles of cyclohexene transformed per number of moles of transition metal per hour), after the first hour of reaction the value of TOF reaches a plateau level characteristic for each catalyst. This fact suggests that there is a constant monotonous increase of the conversion in time. However, even after 7 h reaction time the conversion does not exceed 50% for the most active catalyst $^{2}{}_{\infty}$[$CoCl_2$(4,4′-bpy)] as it can be seen in Fig. 8.

The results plotted in Fig. 8, shows that after 7 h reaction time, there are small differences between the conversion levels and the yields to 1,2-epoxycyclohexane due to the high selectivities for epoxidation (e.g. 88–90%) which are similar for all catalysts, even though the conversion levels are neatly different.

The efficiency of isobutyraldehyde use ($E_{i\text{-}BALD}$) is calculated according to Eq. (4)

$$E_{i\text{-}BALD}(\%) = \frac{n_{i\text{-}BALD\ transformed} - n_{i\text{-}BALD\ consumed\ for\ cyclic\ oxidation\ products}}{n_{i\text{-}BALD\ transformed}} \times 100 \quad (4)$$

where n = number of moles; i-BALD = abbreviation for isobutyraldehyde; $n_{i\text{-}BALD\ transformed} = n_{i\text{-}BALD\ introduced} - n_{i\text{-}BALD\ remaining\ in\ the\ reaction\ mixture}$.

The efficiency of the isobutyraldehyde use is 93% for the catalyst containing Co, and has lower levels for the catalysts containing Cu or Ni which are less active. This fact suggests that, in the case of lower catalytic activities, the isobutyraldehyde is consumed in other secondary reactions than the oxidation of cyclohexene to the corresponding epoxide. The values of the selectivity index (RS) calculated as the ratio between the selectivity to epoxide and the selectivity for cyclohexenol and cyclohexenone express the trend of the oxidation following the pathways (1) or (2) presented in Scheme 2. According to the aspects mentioned by Wentzel et al. [14,30], the double bond oxidation to epoxides is favored by the transition metals that can adopt high oxidation states, while the oxidation in allylic position is specific to metals that adopt lower oxidation states. Therefore it may be understandable why for the Co-containing complex this value is lower than that for Ni or Cu since Co(II) is the lower oxidation state for Co, while Ni(II) and Cu(II) are the higher oxidation states for these metals.

These results prove that the reaction is mainly carried out according to the redox mechanism described in Scheme 3.

Since there is a uniform distribution of the transition metal cations which may act as redox active sites in the structure of the polymeric complexes it would be expected that these compounds possess a high catalytic activity. However, the high thermal and chemical stability of these complexes indicates that most of these transition metal cations are in strong interaction with the corresponding ligands and have a saturated coordination. Therefore, the limited values of the conversion levels may be related to the fact that during the catalytic process only the cations having a non-saturated coordination which are located on the external surface or in the defects of the crystals are involved. Besides, the progressive formation of the isobutyric acid and its desorption rate from the active site could further influence the rather slow evolution of the oxidation.

In an attempt to increase the number of potential active sites in the polymeric complexes, we have investigated the effect of the

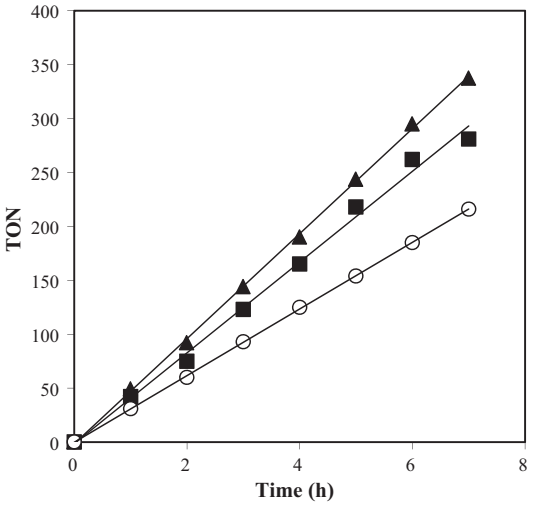

Fig. 9. Temporal variation of the catalytic activity (TON) for $^{2}_{\infty}[CoX_2(4,4'\text{-bpy})]$ catalysts X = Cl ■; X = $(OCOCH_3)$ Δ; X = $C_5H_7O_2$ ○; reaction conditions: 40 mg catalyst, 0.08 mmol cyclohexene, 0.16 mmol isobutyraldehyde, 20 mL acetonitrile solvent, T = 25 °C, p_{O_2} = 1 atm.

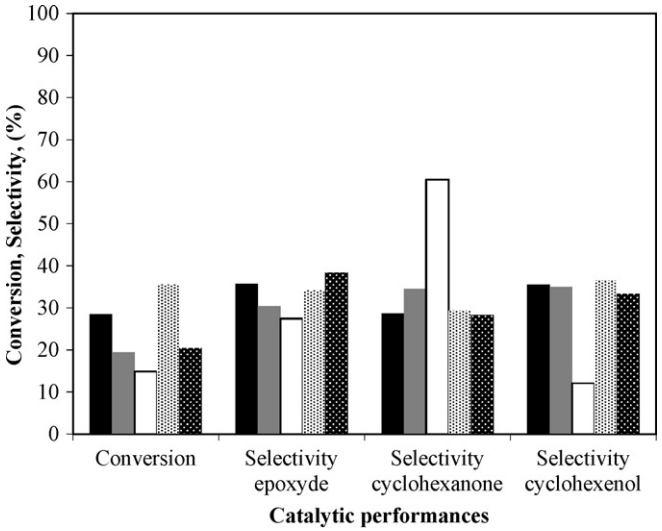

Fig. 11. Catalytic performances of the investigated catalysts in the absence of isobutyraldehyde $^{2}_{\infty}[CoCl_2(4,4'\text{-bpy})]$ ■; $^{2}_{\infty}[NiCl_2(4,4'\text{-bpy})]$ ▩; $^{2}_{\infty}[CuCl_2(4,4'\text{-bpy})]$ □; $^{2}_{\infty}[Co(OCOCH_3)_2(4,4'\text{-bpy})]$ ▨, $^{2}_{\infty}[Co(C_5H_7O_2)_2(4,4'\text{-bpy})]$ ▩ reaction conditions: 40 mg catalyst, 0.08 mmol cyclohexene, 20 mL acetonitrile solvent, 7 h reaction time, T = 25 °C, p_{O_2} = 1 atm.

replacement of chlorine ligands with acetylacetonate or acetate based on the assumption that the interactions of the transition metal cations with these ligands might be weaker and therefore a higher number of sites could be susceptible to participate in the catalytic act. Thus, $^{2}_{\infty}[CoX_2(4,4'\text{-bpy})]$ complexes (X = $OCOCH_3$ or $C_5H_7O_2$) were prepared and their catalytic activity was compared to that of $^{2}_{\infty}[CoCl_2(4,4'\text{-bpy})]$. The obtained results presented in Figs. 9 and 10 show that the nature of the ligand X strongly influences the catalytic activity of $^{2}_{\infty}[CoX_2(4,4'\text{-bpy})]$ complexes while it has a low impact on the selectivity for 1,2-epoxycyclohexane which maintains its high values (88–90%).

The highest catalytic activity is obtained for $^{2}_{\infty}[Co(OCOCH_3)_2(4,4'\text{-bpy})]$ complex which leads to a conversion of about 60% compared to ca. 50% that was obtained with $^{2}_{\infty}[CoCl_2(4,4'\text{-bpy})]$. This complex has the peculiarity that it presents two types of Co(II) sites situated in two independent but similar mononuclear Co(II) moieties as it was revealed by

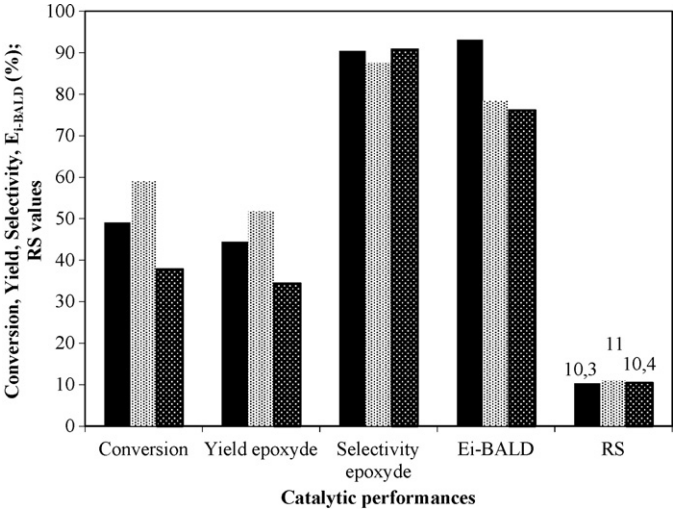

Fig. 10. Catalytic performances of $^{2}_{\infty}[CoX_2(4,4'\text{-bpy})]$ catalysts X = Cl ■; X = $(OCOCH_3)$ ▨, X = $C_5H_7O_2$ ▩ reaction conditions: 40 mg catalyst, 0.08 mmol cyclohexene, 0.16 mmol isobutyraldehyde, 20 mL acetonitrile solvent, 7 h reaction time, T = 25 °C, p_{O_2} = 1 atm.

the XRD studies performed by Zhang et al. [2]. In one of these moieties, the cobalt ion is situated on an inversion center with an octahedral geometry while presenting the specific feature that the Co–O(H_2O) bond lengths are shorter than those in Co–O(acetate) which would be expected to be shorter due to the negative charge of the acetate ion. Zhang attributed this discrepancy of Co–O bond length to Jahn–Teller distortion of a high spin d^7 metal ion. The lower strength of Co–O bond in $^{2}_{\infty}[Co(OCOCH_3)_2(4,4'\text{-bpy})]$ was confirmed by the results of DR-UV–vis NIR analysis. Another explanation regarding the better catalytic activity of $^{2}_{\infty}[Co(OCOCH_3)_2(4,4'\text{-bpy})]$ compared to $^{2}_{\infty}[CoCl_2(4,4'\text{-bpy})]$ can be inferred using the general theory regarding the stability of complex compounds. The concept of hard and soft acids and bases classify Co^{2+} and Cl^- as having an intermediate character while acetate ions and acetylacetonate are hard bases. According to Pearson's rule, the metal ions and ligands of the same class form the most stable complexes, meaning that the complex containing Cl^- ligands will be more stable and therefore the transition metal sites would be less susceptible to undergo modifications of the coordination. The fact that the complex $^{2}_{\infty}[Co(C_5H_7O_2)_2(4,4'\text{-bpy})]$ does not comply with the above mentioned rule, since it has the lowest activity among Co–polymeric complexes, is probably due to its completely different structure as it was revealed by XRD and DR-UV–vis NIR analyses.

It is also interesting to notice that the values of the selectivity index (RS) are not influenced by the nature of the ligands, suggesting that Co ions in all three catalysts are found as Co(II).

In order to highlight the role played by isobutyraldehyde in the process, catalytic tests have been performed using the same reaction conditions (e.g. 40 mg catalyst, 0.08 moles cyclohexene, 20 mL acetonitrile solvent, oxygen pressure 1 atm), without adding isobutyraldehyde. The results displayed in Fig. 11 show that for Co- and Ni-containing catalysts the conversions of cyclohexene were lower than those obtained in the presence of aldehyde, while in the case of Cu catalyst the conversion was unchanged (see also Fig. 8). The lower conversions obtained in this case may be explained by a lower rate of the initiation step of the oxidation. When aldehyde is absent from the reaction system, the first step of the process is the formation of a radical-ion following the adsorption of O_2 on the transition metal sites (Eq. (5)). Then, the interaction of the radical-ion with

Table 5
The results of the leaching tests.

Catalyst	Conversion of cyclo-C_6H_{10} (%)		$Me^{(II)}$ content in the catalyst (%)		$\Delta Me^{(II)}$[b] (%)
	After 7 h	After 14 h[a]	Initial	After 7 h	After 7 h
$^2_\infty[CoCl_2(4,4'\text{-bpy})]$	49.1	54.2	21.04	20.95	0.29
$^2_\infty[Co(OCOCH_3)_2(4,4'\text{-bpy})\times(H_2O)_2]$	59.0	65.3	14.82	14.76	0.27
$^2_\infty[Co(C_5H_7O_2)_2(4,4'\text{-bpy})]$	37.8	41.1	14.54	14.50	0.28
$^2_\infty[NiCl_2(4,4'\text{-bpy})]$	36.9	40.5	21.10	21.05	0.24
$^2_\infty[CuCl_2(4,4'\text{-bpy})]$	16.4	21.2	22.30	22.23	0.27

[a] Refers to the conversion obtained after the supplementary 7 h in the absence of the catalyst.
[b] $\Delta Me^{(II)}\,(\%) = (Me^{(II)}_{initial} - Me^{(II)}_{after\ 7\ h}) \times 100/Me^{(II)}_{initial}$.

the hydrocarbon generates free radicals (Eq. (6)) which are further combined to give the alkyl-hydroperoxide (Eq. (7)) [41].

$$[]\text{-}M^{2+} + O_2 \leftrightarrow []\text{-}[M^{3+}\cdots O^{\bullet}\text{–}O^{-}]^{2+} \quad (5)$$

$$[] - [M^{3+}\cdots O^{\bullet} - O]^{2+} \xrightarrow{RH} [] - M^{2+} + R^{\bullet} + HO^{\bullet}{}_2 \quad (6)$$

$$R^{\bullet} + HO_2{}^{\bullet} \rightarrow ROOH \quad (7)$$

The formation of the radical ion in Eq. (5) is possible for Co and Ni catalysts since these transition metals can exist in both oxidation states. Meanwhile, for the copper containing catalyst this mechanism cannot be applied since Cu(II) is the higher oxidation state and this fact may explain why the conversion of cyclohexene did not vary in this case.

The selectivities for 1,2-epoxyxyclohexane were less than half of the values obtained in the presence of aldehyde for all catalysts, suggesting that the presence of aldehyde is critical for the formation of this product. The copper polymeric complex seemed to be the most selective for the obtaining of cyclohexenone which is an allylic oxidation product. This fact confirmed that the oxidation in allylic position is specific to copper complexes even in the absence of isobutyraldehyde [7].

The results of the catalytic tests performed in order to highlight the leaching of the catalysts are presented in Table 5. These data show that there is no leaching of Me(II) ions after one reaction cycle since the differences between the concentration of metal before and after the catalytic test are less than 0.5%. The slow increase in the conversion of cyclohexene after another 7 h in the absence of the catalyst is most likely due to a usual non-catalytic oxidation taking into account the results of the blank tests which showed that cyclohexene conversion may reach 10.1% after 7 h. The fact that leaching is absent is also confirmed by the results presented in Fig. 12 showing the constant level of cyclohexene conversion obtained when the catalysts were tested in 5 consecutive reaction cycles.

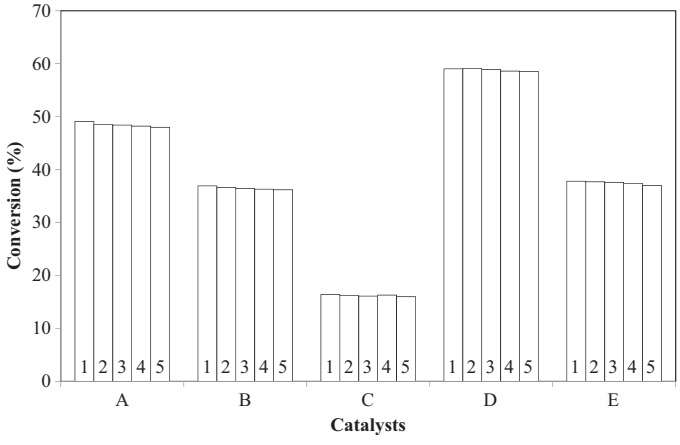

Fig. 12. Variation of cyclohexene conversion during 5 reaction cycles. Catalysts: A – $^2_\infty[CoCl_2(4,4'\text{-bpy})]$, B – $^2_\infty[NiCl_2(4,4'\text{-bpy})]$, C – $^2_\infty[CuCl_2(4,4'\text{-bpy})]$, D – $^2_\infty[Co(OCOCH_3)_2(4,4'\text{-bpy})]$, E – $^2_\infty[Co(C_5H_7O_2)_2(4,4'\text{-bpy})]$. Reaction conditions: 400 mg catalyst, 0.8 mmol cyclohexene, 200 mL acetonitrile solvent, 7 h reaction time for each cycle, $T = 25\,^\circ C$, $p_{O_2} = 1$ atm, number of cycles 1–5.

The good stability and the recyclability of all the transition metal polymeric complexes were also confirmed by the results of XRD analysis.

4. Conclusions

Based on the obtained results it may be concluded that the chemical binding of $Me(II)X_2$ (Me(II) = Co, Ni, Cu; X = Cl, $(OCOCH_3)$, $(C_5H_7O_2)$) in a complex polymeric structure with 4,4′-bpy bridging ligands provides an opportunity to obtain structures that have no soluble correspondents and that these metals and ligands can also work as catalysts in coordination polymers improving the selectivity for the epoxidation of cyclohexene with molecular oxygen and isobutyraldehyde. These catalysts present the advantage of a high stability and may be recycled in several reaction cycles without the alteration of their structure. The catalytic activity of these complexes is especially influenced by the nature of the transition metal cation and the nature of the ligand X. The complex containing Co(II) cations and acetate as ligand X presents the highest catalytic activity. This fact could probably be related to the lower strength of the bonds between acetate ligand and the transition metal cation which may result in coordination defects in the structure leading to an increase of the number of potential active sites.

References

[1] M.A. Lawandy, X. Huang, R.-J. Wang, J. Li, J.Y. Lu, T. Yuen, C.L. Liu, Inorg. Chem. 38 (1999) 5410–5414.
[2] Y.-S. Zhang, G.D. Enright, S.R. Breeze, S. Wang, New J. Chem. 23 (1999) 625–628.
[3] O.M. Yaghi, H. Li, T.L. Groy, Inorg. Chem. 36 (1997) 4292–4293.
[4] J. Chakraborty, M. Nandi, H. Mayer-Figge, W.S. Sheldrick, L. Sorace, A. Bhaumik, P. Banerjee, Eur. J. Inorg. Chem. (2007) 5033–5044.
[5] M.R. Maurya, A. Kumar, J. Mol. Catal. A: Chem. 250 (2006) 190–198.
[6] K. Brown, S. Zolezzi, P. Aguirre, D. Venegas-Yazigi, V. Paredes-García, R. Baggio, M.A. Novak, E. Spodine, Dalton Trans (2009) 1422–1427.
[7] S.M. Islam, P. Mondal, S. Mukherjee, A.S. Roy, A. Bhaumik, Polym. Adv. Technol. 22 (2011) 933–941.
[8] H.H. Monfared, A. Mohajeri, A. Morsali, C. Janiak, Monatsh. Chem. 140 (2009) 1437–1445.
[9] C. Vartzouma, E. Evaggellou, Y. Sanakis, N. Hadjiliadis, M. Louloudi, J. Mol. Catal. A: Chem. 263 (2007) 77–85.
[10] M.R. Maurya, A. Arya, P. Adão, J.C. Pessoa, Appl. Catal. A: Gen. 351 (2008) 239–252.
[11] Z. Lei, X. Han, Y. Hu, R. Wang, Y. Wang, J. Appl. Polym. Sci. 75 (2000) 1068–1074.
[12] D.M. Jiang, T. Mallat, D.M. Meier, A. Urakawa, A. Baiker, J. Catal. 270 (2010) 26–33.
[13] T. Mukaiyama, Aldrichim. Acta 29 (1996) 59–76.
[14] B.B. Wentzel, P.A. Gosling, M.C. Feiters, R.J.M. Nolte, J. Chem. Soc. Dalton Trans. 224 (1998) 1–2246.
[15] N. Fdil, A. Romane, S. Allaoud, A. Karim, Y. Castanet, A. Mortreux, J. Mol. Catal. A: Chem. 108 (1996) 15–21.
[16] P.M. O'Neill, S. Hindley, M.D. Pugh, J. Davies, P.G. Bray, B.K. Park, D.S. Kapu, S.A. Ward, P.A. Stocks, Tetrahedron Lett. 44 (2003) 8135–8138.
[17] T. Takai, E. Hata, K. Yorozu, T. Mukaiyama, Chem. Lett. 207 (1992) 7–2080.
[18] J.T. Groves, R. Quinn, J. Am. Chem. Soc. 107 (20) (1985) 5790–5792.
[19] V. Kesavan, S. Chandrasekaran, J. Chem. Soc. Perkin Trans. 1 [old] (1997) 3115–3116.

[20] Y.-J. Ye, X.-T. Zhou, J.-W. Huang, J.-H. Cai, W.-H. Wu, H.-C. Yu, H.-B. Ji, L.-N. Ji, J. Mol. Catal. A: Chem. 331 (2010) 29–34.
[21] A. Pramanik, S. Abbina, G. Das, Polyhedron 26 (2007) 5225–5234.
[22] E. Angelescu, R. Ionescu, O.D. Pavel, R. Zăvoianu, R. Birjega, C.R. Luculescu, M. Florea, R. Olar, J. Mol. Catal. A: Chem. 315 (2010) 178–186.
[23] JCPDS-International Centre for Diffraction Data, PDF4+ (2009).
[24] N. Masciocchi, P. Cairati, L. Carlucci, G. Mezza, G. Ciani, A. Sironi, J. Chem. Soc. Dalton Trans. 273 (1996) 9–2746.
[25] R.D. Shannon, Acta Crystallogr. A32 (1976) 751–767.
[26] R. Feyerherm, A. Loose, M.A. Lawandy, J. Li, Appl. Phys. A 74 [Suppl.] (2002) S778–S780.
[27] E. König, Struct. Bond. 9 (1972) 185–187.
[28] A.B.P. Lever, Inorganic Electronic Spectroscopy, Elsevier, Amsterdam, London, New York, 1986, pp. 480–487, 507–510, 555–560.
[29] L. Sacconi, F. Mani, A. Bemcini, B.J. Hathaway, in: G. Wilkinson, R.D. Gillard, J.A. McCleverty (Eds.), Comprehensive Coordination Chemistry, vol. 5, first ed., Pergamon Press, Oxford, UK, 1987, pp. 45–55, 652–656.
[30] B.B. Wentzel, P.L. Alsters, M.C. Feiters, R.J.M. Nolte, J. Org. Chem. 69 (2004) 3453–3464.
[31] W. Nam, H.J. Kim, S.H. Kim, R.Y.N. Ho, J.S. Valentine, Inorg. Chem. 35 (1996) 1045–1049.
[32] K. Kaneda, S. Haruna, T. Imanaka, M. Hamamoto, Y. Nishiyama, Y. Ishii, Tetrahedron Lett. 33 (1992) 6827–6830.
[33] K.R. Lassila, F.J. Waller, S.E. Werkheiser, A.L. Wressell, Tetrahedron Lett. 35 (1994) 8077–8080.
[34] T. Nagata, K. Imagawa, T. Yamada, T. Mukaiyama, Bull. Chem. Soc. Jpn. 68 (1995) 3241–3246.
[35] T. Mukaiyama, T. Yamada, T. Nagata, K. Imagawa, Chem. Lett. 22 (1993) 327–330.
[36] E. Hata, T. Takai, T. Yamada, T. Mukaiyama, Chem. Lett. 23 (1994) 535–538.
[37] T. Yamada, K. Imagawa, T. Mukaiyama, Chem. Lett. 21 (1992) 2109–2112.
[38] T. Yamada, K. Imagawa, T. Nagata, T. Mukaiyama, Chem. Lett. 21 (1992) 2231–2234.
[39] N. Mizuno, H. Weiner, R.G. Finke, J. Mol. Catal. A: Chem. 114 (1996) 15–28.
[40] M.V. Patil, M.K. Yadav, R.V. Jasra, J. Mol. Catal. A: Chem. 277 (2007) 72–80.
[41] A.D. Pomogailo, Kinet. Catal. 45 (2004) 61–103.